

Fig.3 Switched CW charge pump unit

rather similar, and are based on charge pump design incorporating only capacitors and switches instead of diodes or diode connected MOSFETs. Those designs require up to four non-interleaving clock signals in order to operate switches, which must be able to completely turn off and on in order to ensure the proper charge pump operation [8], [9].

In this paper we propose a version of switched Cockcroft-Walton (SCW) charge pump for driving capacitive loads. The design is fairly simple. The charge pump requires only the AC signal, with  $V_m$  greater than  $V_{Tn}$ , which can be sine or square wave, as opposed to majority of reported charge pumps which require DC voltage and/or special clocking schemes [10]-[17]. No DC voltage is needed for this charge pump, what makes this charge pump suitable for usage in RFID tags, where only the RF signal is available for DC voltage generation.

## 2 Switched CW Charge Pump

In the switched CW charge pump two regular pumping stages are merged into one major pumping unit which, when modeled with diodes and switches, consists of 2 capacitors, 2 diodes and 2 switches, as shown on Fig.2. There are two operational states for this charge pump. In first, while switch S1 is closed and S2 opened, the

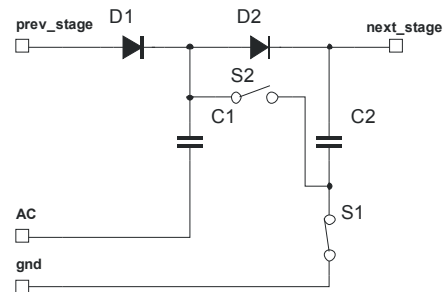


Fig.2 Switched CW charge pump unit modeled with diodes and switches

charge pump charges as ordinary CW charge pump. In second state, when switch S1 is opened and S2 closed, the charge unit capacitors C1 and C2 are through switch S2 connected serially and the voltage passed to the next pumping unit is significantly higher.

The full charge pumping unit schematics is shown in Fig.3. Due to better clarity of the schematics, the connections between ground and the body of each MOSFET are not shown. M1 and M2 are diode connected MOSFETs which with capacitors C1 and C2 form a regular CW charge pump. MOSFETs M3 and M4 are used as switches S1 and S2, respectively. Two additional MOSFETs M5 and M6, are added to ensure that M4 (switch S2) can be completely turned on and off. In fact, M5 and M6 form an inverter driving stage for MOSFET M4, where the active load resistor M5 is made of a long MOSFET, keeping the power consumption minimal.

## 2.1 Charging phases

As mentioned before, the presented charge pump has two operational phases. The regular Cockcroft-Walton charging phase and switched charging phase. When M6 is turned on, the gate of the M4 is connected to the ground, thus M4 is turned off. When M6 is turned off, the voltage level of capacitor C1 is through M5 brought to the gate of the M4, hence turning it on.

This way, when AC signal is positive, the M3 and M6 are turned on, and the M4 is turned off. This is first operational state in which the charge pump charges as regular CW charge pump. When AC drops to its negative value, the MOSFETs M3 and M6 are turned off, M4 is turned on, and charge pump is in the second operational phase where the heaped voltage (serially connected) from capacitors C1 and C2 is passed on the output of the pumping unit.

## 2.2 Mathematical formulation

The SCW charge unit has two charging phases. Mathematical formulation for obtaining the voltage which is transferred to the next stage must be calculated with respect to both phases. The equations bellow are giving the maximal voltage values which describe the stationary conditions for fully charged pump.

$$V_{C1} = V_{prev\_stage} - V_{TnM1} \quad (2)$$

where  $V_{C1}$  is capacitor C1 voltage,  $V_{prev\_stage}$  is heaped voltage from previous SCW unit, and  $V_{TnM1}$  is threshold voltage for diode connected MOSFET M1.

$$V_{C2} = V_{C1} + V_{AC} - V_{TnM2} - V_{TnM3} \quad (3)$$

where  $V_{C2}$  is capacitor C2 voltage,  $V_{AC}$  is supply voltage, and the  $V_{TnM2}$  and  $V_{TnM3}$  are the threshold voltages of diode connected MOSFET M2 and switch M3, respectively.

$$V_{next\_stage} = V_{C1} + V_{C2} - V_{TnM4} \quad (4)$$

where  $V_{next\_stage}$  is heaped voltage from capacitors C1 and C2 which is transferred to the next stage, basically SCW unit's output voltage, and  $V_{TnM4}$  is threshold voltage for switch M4.

The final expression for SCW unit's output voltage is given by (5).

$$V_{next\_stage} = 2 \cdot V_{prev\_stage} + V_{AC} - 2 \cdot V_{TnM1} - V_{TnM2} - V_{TnM3} - V_{TnM4} \quad (5)$$

Since every pumping unit added to the charge pump raises the output voltage much faster than the regular CW charge pump the body effects of later MOSFET's are more expressed. The following equation gives the mathematical formulation [18] for threshold voltage  $V_{Tn}$  when body effect is present.

$$V_{Tn} = V_{Tn0} + \Delta V_{Tn} \quad (6)$$

where the  $V_{Tn0}$  is the threshold voltage of MOSFET with no body effect present, and  $\Delta V_{Tn}$  is the threshold variation given as a function of source-body voltage  $V_{sb}$ , as shown in (7).

$$\Delta V_{Tn} = \gamma \left( \sqrt{2|\Phi_p| + V_{sb}} - \sqrt{2|\Phi_p|} \right) \quad (7)$$

where the  $\gamma$  and  $\Phi_p$  are further explained in (8) and (9), respectively.

$$\gamma = \frac{\sqrt{2\varepsilon_s q N_a}}{C_{ox}} \quad (8)$$

$$\Phi_p = -\frac{KT}{q} \ln \left( \frac{N_a}{n_i} \right) \quad (9)$$

By cascading the SCW charge pump units a SCW charge pump with any even number of stages can be made, as shown in Fig.3. The output voltage of such an arrangement can be calculated using equations (2)-(9).

### 3 Simulation

Simulation of the switched CW charge pump is done with Multisim 2001® software, using 0.35 $\mu$ m n-well CMOS level 49 SPICE models [19].

In the comparison between CW and SCW charge pump, the number of pumping stages is one of the parameters. Basically, the number of stages is equal to the number of capacitors in the charge pump, without the output stage. The SCW charge pump consists of charge pump units which are two pumping stages merged together. This is the reason why only the charge pumps with even number of stages were simulated.

By increasing the number of pumping stages, the voltage increases accordingly. For exclusively capacitive load, with no parallel resistive load applied to the output capacitor, comparison between output voltages of the SCW and CW charge pump, for a different number of pumping stages, and different values of the pumping capacitors, is given in Fig.4. The typical capacitance values for pumping capacitors in related papers [1]-[17] vary from 1pF up to 30 nF.

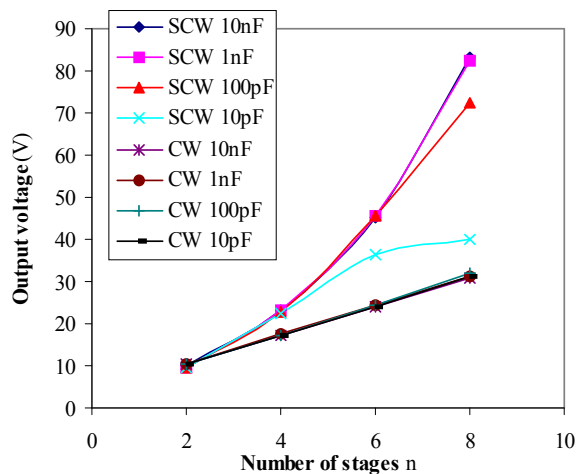


Fig.4 Output voltage comparison for SCW and CW charge pump for a different number of pumping stages, and different values of the pumping capacitors,  $V_{AC}=3.5V$ .

For SCW with 10 pF pumping capacitors can be seen the output voltage drop for 8-stage charge pump caused by power consumption of the additional MOSFETs added to the charge pump units. This same voltage drop can be observed for SCW pump with 100pF capacitors, but in smaller scale. This voltage drop is directly caused by consumption of the inverter drive stage, where during CW charging phase, the first capacitor in SCW unit is discharging through active load resistor in inverter. That output voltage drop problem can be solved by using larger pumping capacitors or using higher frequency for AC supply voltage source.

### 3.1 Output characteristics

The output characteristics  $V_{out}$  vs.  $I_{out}$  of the SCW and CW charge pump are compared. The both charge pumps are 8-stage charge pumps with 10 pF, 100 pF, 1 nF, and 10 nF capacitors, and the frequency of the AC supply is set to the 1 MHz sine wave. Amplitude of the AC supply voltage is set to 3.5 V. Results of the comparison are given in Fig.5.

The SCW charge pump is designed to work under capacitive or low current load. For that reason the output currents in Fig.5 are given in logarithmic scale, which gives better overview of the low current region.

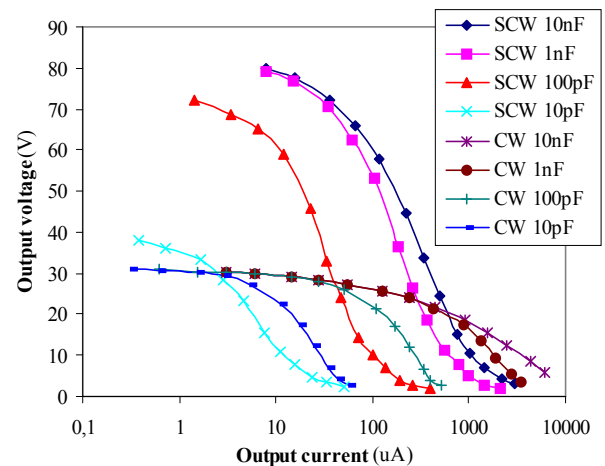


Fig.5 Output voltages of the 8-stage SCW and CW charge pump under different output currents, logarithmic scale,  $V_{AC}=3.5V$

### 3.2 Charging time

The significant factor in charge pumps which are used in indirectly powered circuits is the charging time. The charging times of the SCW charge pump presented in this paper and CW charge pump are compared, and the result are given in Table 1. Note that the charging time values in Table 1 are time values needed for a certain charge pump to reach the 90% of its maximal output voltage which is much higher for SCW charge pump.

For better comparison between charge pumps Table 2 shows output voltage values for SCW and CW charge pump for charging time in which CW reaches 90% of its maximal output voltage value. The results in Table 2 show us that the SCW charge pump has improved performance also when the charging time is taken into consideration.

TABLE 1  
CHARGING TIME FOR 90% OF MAXIMAL OUTPUT VOLTAGE [ $\mu\text{s}$ ]

Number of stages $n$	10pF		100pF		1nF		10nF	
	CW	SCW	CW	SCW	CW	SCW	CW	SCW
2	7.2	11	9.3	19	31	82	320	1200
4	19	36	27	55	98	268	840	2400
6	42	90	52	150	177	465	1300	3500
8	72	138	99	408	260	1000	2000	7500

TABLE 2  
OUTPUT VOLTAGES FOR SCW AND CW CHARGE PUMP FOR CHARGING TIME IN WHICH CW REACHES 90% OF ITS MAXIMAL OUTPUT VOLTAGE VALUE,  $V_{AC}=3.5\text{V}$

Number of stages $n$	10pF		100pF		1nF		10nF	
	CW	SCW	CW	SCW	CW	SCW	CW	SCW
2	9.4	7.7	9.7	7.4	9.3	7.5	9.4	8.1
4	15.5	16.3	15.7	16.8	15.8	18.7	15.7	18.8
6	21.8	24.7	22	25.9	22	33.6	21.6	34
8	28.3	30	28.9	35.7	28	46	27.8	52

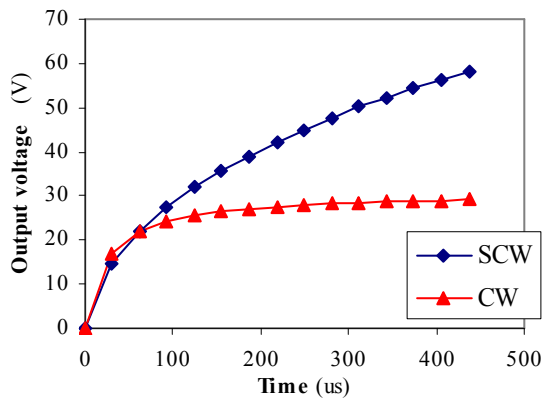


Fig.6 Output voltages in the charging process for 8-stage SCW and CW charge pump with 1nF pumping capacitors,  $V_{AC}=3.5\text{V}$ .

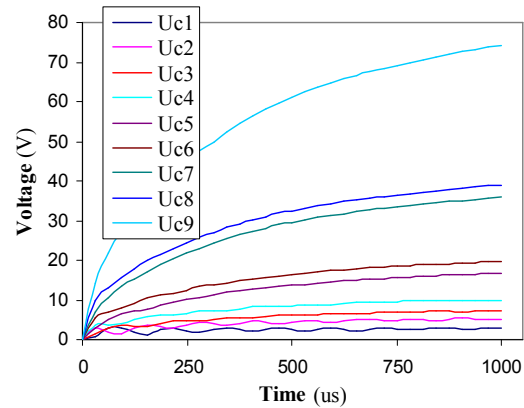


Fig.7 Pumping capacitors voltages in the charging process for 8-stage SCW charge pump with 1nF pumping capacitors,  $V_{AC}=3.5\text{V}$ .

The charging processes for 8-stage SCW and CW charge pumps with 1nF pumping capacitors are given by Fig.6. Both charge pumps have approximately the same charging time (CW slightly better) until the CW reaches 70% of its maximal output voltage. After that the CW pump slows down charging toward its lower output voltage, and SCW continues charging much quicker.

### 3.3 Capacitors voltage levels

With respect to the CW, the SCW charge pump's capacitors are charging with larger steps between SCW units. This can be observed in Fig.7, where the charging process for capacitors in a 8-stage SCW pump is presented. Each two curves that are placed close to each other are from two capacitors that are forming one SCW

unit. The following pair of the curves represent the capacitors from the next SCW unit. It can be seen that there is a significant jump in voltage value that comes from switched operational mode presented in this charge pump.

### 3.4 Node voltage waveforms

Node are representing the higher potential points of each capacitor in a charge pump. Since the low potential point of each capacitor changes with AC supply signal phases, for a CW charge pump, and also during switched charging phase in SCW charge pump. Node voltage waveforms are a good way, beside the capacitor voltages, to observe the charging process. The difference is that node voltage give us insight to voltage oscillations between charge pump stages.

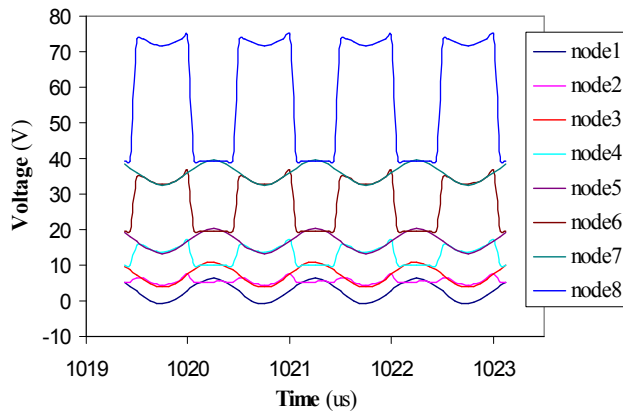


Fig.8 Node voltages for 8-stage SCW charge pump with 1nF pumping capacitors,  $V_{AC}=3.5V$ .

The charge pump node voltages are given by Fig.8. Every second waveform corresponds to a certain charging phase. The sine waveforms are corresponding to the ordinary CW charging, and the almost square waveforms with significant amplitude boosts are corresponding to the switched charging phase, where the heaped voltage from both capacitors in a SCW unit is charging the following stage.

### 3.5 Overstress voltage conditions

Due to switched operational mode used in this charge pump, the main MOSFET switches, diode connected MOSFETs and inverter circuit are to experience overstress voltage. Voltage waveforms on charge pump's switches are crucial for proper operation of the circuit. Following figures are showing the voltage waveforms on switches S1 and S2, Diode connected MOSFETs D1 and D2, and inverter circuits, respectively.

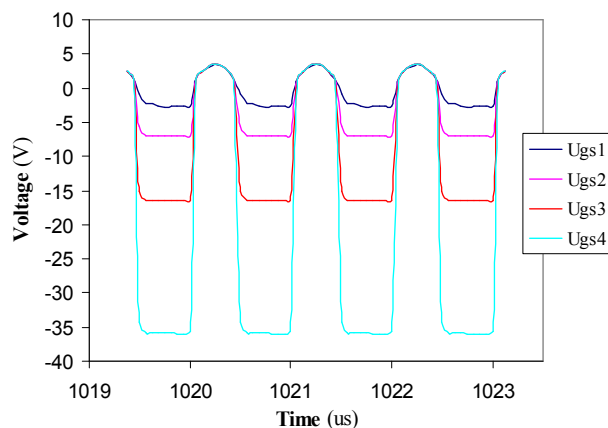


Fig.9 Switch S1 Ugs voltages for 8-stage SCW charge pump with 1nF pumping capacitors,  $V_{AC}=3.5V$ .

Fig.9 shows the Ugs voltage for switch S1. Numbers in labels in the chart legend represent the SCW unit for which the Ugs voltage of switch S1 is given. When closed switch S1 enables the CW charging phase. It is important that this switch can be fully turned off in order to eliminate the possibility of charge leakage through this switch when the pump is in switched charging phase. This is accomplished by using the AC signal for switching between charging phases.

When the switch S1 is „on“, the positive half-period of the AC signal is brought to the it's gate. When the switch must go in „off“ state, the voltage from this unit's first capacitor is through S2 brought to it's source so the Ugs voltage goes deep in the negative region. This effect is more expressed an later stages, where also more charge on single capacitor is present.

Fig.10 shows the waveforms for the Ugs voltage of the switch S2. This switch is connected to the rest of the circuit in two ways, depending on the charging phase. In CW charging phase the switch has gate connected to the ground through the inverter driving stage. While in switched charging phase, it's gate is through active resistor M5 connected to it's drain. Due to high resistivity of M5, and very small consumption of the inverter driving stage, switch S2 basically becomes a diode connected MOSFET with  $U_{gd}=0$ . This is essential because in the switched charging phase it's source is disconnected from the AC supply (switch S1 is „off“), making it a „floating“ node in circuit. A diode connected MOSFET is the one solution that worked in this case, since the restriction was not to use any additional control signals.

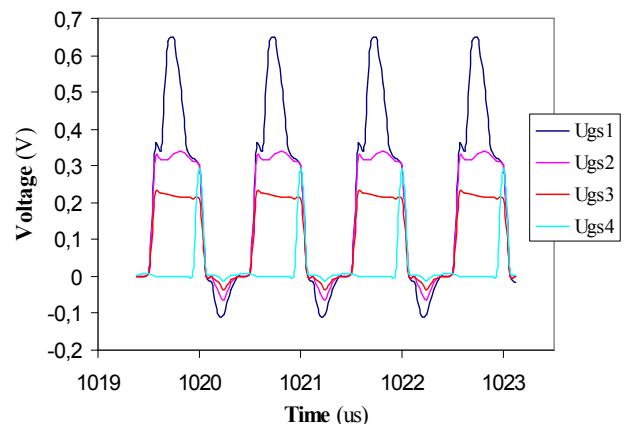


Fig.10 Switch S2 Ugs voltages for 8-stage SCW charge pump with 1nF pumping capacitors,  $V_{AC}=3.5V$ .

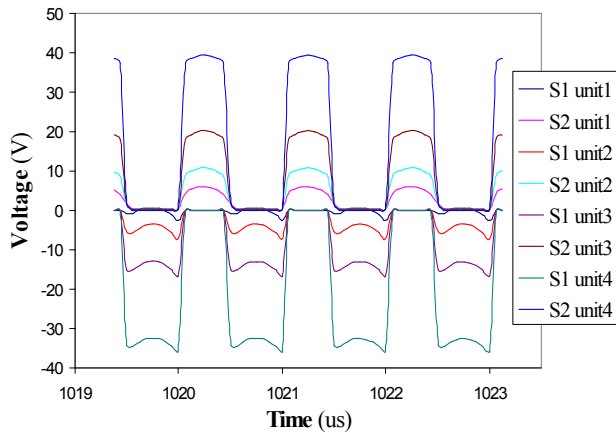


Fig.11 Uds voltages for switches S1 and S2 of the 8-stage SCW charge pump with 1nF pumping capacitors,  $V_{AC}=3.5V$ .

Fig.11 shows the Uds voltages for switches S1 and S2. The waveforms for both switches are given in the same figure in order to show two charging phases present in our pump. There are 8 traces in the Fig.11, each representing a switch in a 8-stage SCW charge pump arrangement. All S1 and S2 switches from charge pump units are simultaneously opening and closing, thus flipping between charging phases. The later stages in this arrangement experience more overstress voltage across drain-source region, so that has to be taken into account when choosing the desired number of stages, and must be in concordance with MOSFET specifications.

The Ugd voltage waveform for switch S2 is given in Fig.12. Switch S2, as mentioned before, becomes a diode connected MOSFET in switched charging phase. That can be observed in this figure. When S2 is diode connected the Ugd voltage should drop to 0V. The traces in figure are showing that this is the case for later stages, where the good charge transfer is required, while in the first stages Ugd voltage has peak value of 0,7V.

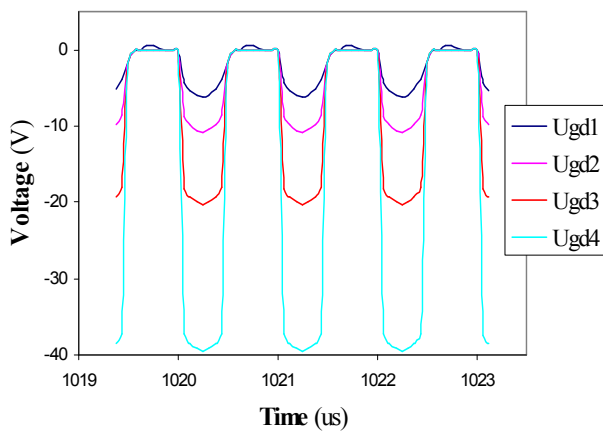


Fig.12 Ugd voltages for switch S2 of the 8-stage SCW charge pump with 1nF pumping capacitors,  $V_{AC}=3.5V$ .

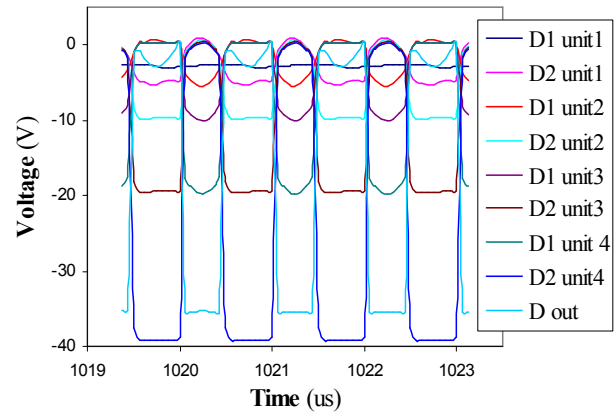


Fig.13 Uds voltages for diode-connected MOSFET's of the 8-stage SCW charge pump with 1nF pumping capacitors,  $V_{AC}=3.5V$ .

Fig.13 shows the Uds voltage waveforms for diode-connected MOSFET's which are forming the CW part of the presented charge pump. Also, as by the Uds voltages on switches S1 and S2, there are significant voltage level jumps with each SCW unit, and overstress voltage is expected for later stages of the charge pump.

Fig.14 shows the Uds voltage waveforms for the active load resistor in the inverter driving stage. Time intervals when voltage drops to 0V, are the switched charging phases, and the time intervals when there is voltage present on resistor, are the CW charging phase. Active resistor must be a long MOSFET, because in CW charging phase, the voltage across resistor is through it directly connected to the ground. And with long MOSFET the power consumption and charge loss of the inverter driving stage is kept minimal. As before, with more stages added the voltage across resistor raises.

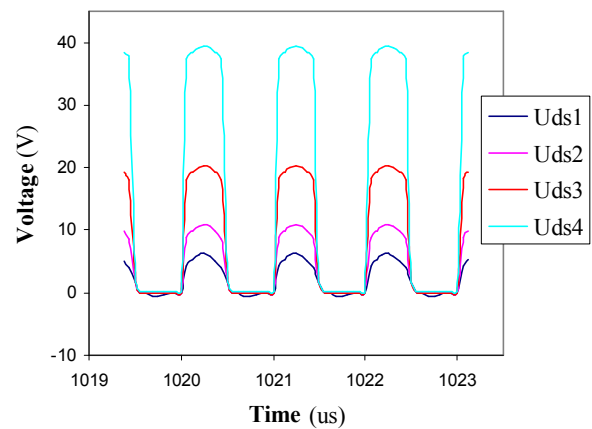


Fig.14 Uds voltages for active load resistor in inverter driving stage of the 8-stage SCW charge pump with 1nF pumping capacitors,  $V_{AC}=3.5V$ .

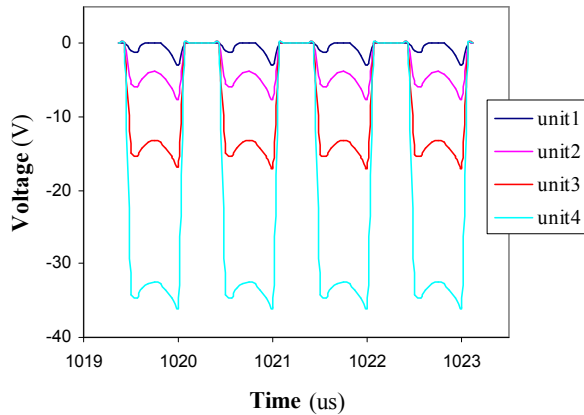


Fig.15 Uds voltages for switch in inverter driving stage of the 8-stage SCW charge pump with 1nF pumping capacitors,  $V_{AC}=3.5V$ .

Fig.15 gives us the Uds voltages for switch in inverter driving stage in each SCW unit of the 8-stage charge pump. In comparison with Fig.14, you can see that they are complementary, what is consistent with their inverter function.

### 3.6 Body effect conditions

The body effect is the reason for the rise of the threshold voltage due to source-body voltage  $U_{sb}$ . And that leads to lower output voltage. Presented charge pump uses n-well MOS structure, which gives the worst case scenario for body effect. The following Figures are showing the  $U_{sb}$  voltage waveforms on MOSFETs in the 8-stage SCW charge pump.

The circuit is designed in such manner that switches S1 and S2 have connected sources. For that reason, the S1 and S2  $U_{sb}$  voltages, in the same SCW unit, are equal. This poses a problem for switch S2, because in

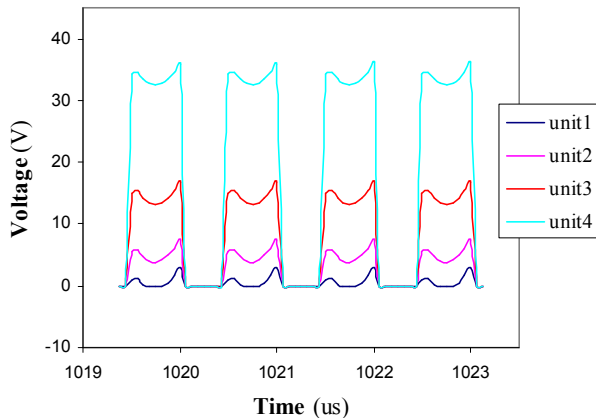


Fig.16  $U_{sb}$  voltages for switches S1 and S2 of the 8-stage SCW charge pump with 1nF pumping capacitors,  $V_{AC}=3.5V$ .

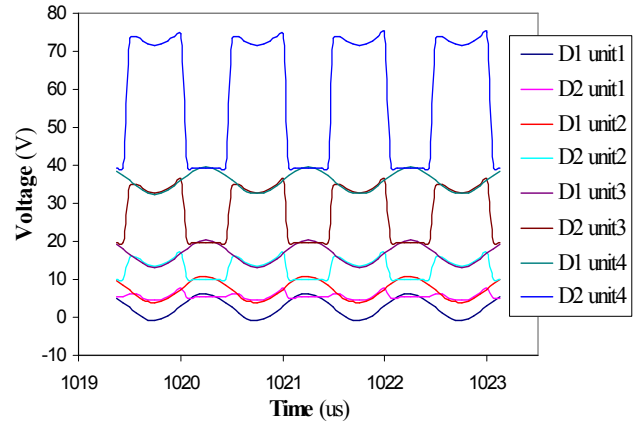


Fig.17  $U_{sb}$  voltages for diode connected MOSFET's of the 8-stage SCW charge pump with 1nF pumping capacitors,  $V_{AC}=3.5V$ .

the switched charging phase S2 in under maximal  $U_{sb}$  voltage, resulting in maximal body effect for a switch. The positive side is that in the same time, switch S2 has the same body effect condition, making the charge leakage through even less possible, with respect to conditions explained in Fig.9. Also, in CW charging phase, switch S2 is under no influence of body effect, allowing easier CW charging phase.

Fig.17 shows the  $U_{sb}$  voltages for diode connected MOSFET's forming a standard CW charge pump. The body effects on those MOSFET's are more expressed with each following stage. This is the effect which cannot be avoided with common CW charge pump structure. The only difference to a regular CW charge pump is that in SCW charge pump body effect becomes more expressed faster, then in CW charge pump. But that is in concordance with improved performance of SCW pump which supplies higher output voltages with less stages used.

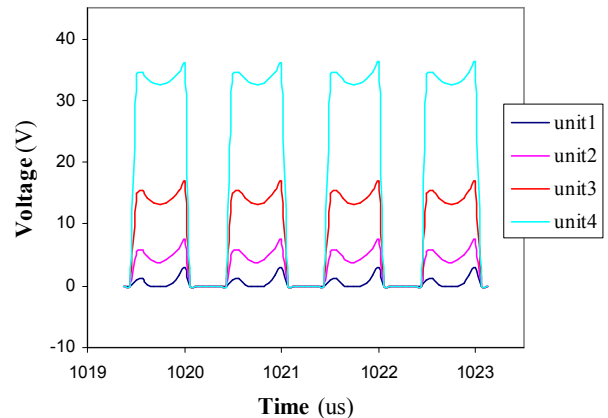


Fig.18  $U_{sb}$  voltages for active load resistor in inverter driving stage of the 8-stage SCW charge pump with 1nF pumping capacitors,  $V_{AC}=3.5V$ .

Fig.18 shows the source-body voltage waveforms for active resistor used in inverter driving stage for each unit in the 8-stage SCW charge pump. Resistor is diode connected, and its dimensions are providing a low consumption for this part of the circuit. For that reason, the body effect is not a crucial parameter for it to function properly. However, during the switched charging phase, there is body effect present, while during CW charging phase there is no body effect on active resistor. These same voltage waveforms are present on switches S1 and S2.

MOSFET switch (M6 in Fig.3.) in inverter driving stage is the only element in this circuit with source always connected to the ground, thus with no body effect present during both operational phases.

#### 4 Conclusion

The design we showed offers great save in number of capacitors needed for desired output voltage. It uses simple design with no additional control signals and clocking schemes needed. The AC power supply which is present in a regular Cockcroft-Walton charge pump is now used to its full extend by using it as control signal for operating two charging phases presented in Switched Cockcroft-Walton (SCW) charge pump. Not only that this way we have reduced the complexity of circuit to minimum, but also we have made sure that our control signals (positive and negative half-period of sine wave) are non-overlapping signals. Also, we have used n-well MOS structure, which is the worst we could use, in terms of body effect conditions charge pump was under. But even under such restrictions, the presented charge pump design has shown outstanding performance. To match the 8-stage SCW charge pump characteristics the CW charge pump would have to be at least 24-stage pump. This means that 2/3 of CW pumping capacitors can now be removed without decreasing the output voltage, what offers great chip area saving. SCW charge pump has shown improved performance in charging time also. The problem with this design is overstress voltage, and that gets more expressed with each new SCW charging unit added to the pump. So that desired number of charge pump stages, expected overstress voltage and MOSFET specifications must match. Drawback of the SCW charge pump is that it cannot cope with CW charge pump when higher currents are needed, what is expected since it is designed for driving capacitive loads. And the best results of SCW charge pump are expected in driving low current circuits, preferably capacitive loads, and indirectly powered circuits.

#### References:

- [1] J. S. Witters, G. Groesenken, and H. E. Maes, "Analysis and modeling of on-chip high-voltage generator circuits for use in EEPROM circuits," *IEEE Journal of Solid-state Circuits*, vol. 24, No. 5, October 1999, pp. 1372-1380.
- [2] K. Eguchi, T. Inoue, I. Oota, H. Zhu, and F. Ueno, "A Cross-Coupled Type AC-DC Converter for Remote Power Feeding to a RFID Tag," *WSEAS Transactions on Circuits and Systems*, Issue 11, vol. 6, November 2007, pp. 592-600.
- [3] F. Kocer and M. P. Flynn, "A new transponder architecture with on-chip ADC for long-range telemetry applications," *IEEE Journal of Solid-state Circuits*, vol. 41, No. 5, May 2006, pp. 1142-1148.
- [4] J. Colomer, A. Saiz-Vela, P. Miribel, M. Viladoms, M. Puig-Vidal, and J. Samitier, "Efficient low-voltage low-power Converters or Self Powered Microsystems (SPMS) based on 0.13 $\mu$ m," *WSEAS Transactions on Electronics*, Issue 4, vol. 3, April 2006, pp. 150-155.
- [5] T. Tanzawa and S. Atsumi, "Optimization of word-line booster circuits for low-voltage flash memories," *IEEE Journal of Solid-state Circuits*, vol. 34, No. 8, August 1999, pp. 1091-1098.
- [6] J.-s. Kim and S. Kim, "High voltage generator using a heap-pump circuit for low voltage embedded FLASH memories," *Journal of the Korean Physical Society*, vol. 41, No. 4, October 2002, pp. 468-470.
- [7] T. Tanzawa, T. Tanaka, K. Takeuchi, and H. Nakamura, "Circuit techniques for a 1.8-V-only NAND flash memory," *IEEE Journal of Solid-state Circuits*, vol. 37, No. 1, January 2002, pp. 84-89.
- [8] L. S. Y. Wong, S. Hossain, A. Ta, J. Edvinsson, D.H. Riva, and H. Nääs, "A very low-power CMOS mixed-signal IC for implantable pacemaker applications," *IEEE Journal of Solid-state Circuits*, vol. 39, No. 12, December 2004, pp. 2446-2456.
- [9] C. Lauterbach, W. Weber, and D. Römer, "Charge sharing concept and new clocking scheme for power efficiency and electromagnetic emission improvement of boosted charge pumps," *IEEE Journal of Solid-state Circuits*, vol. 35, No. 5, May 2000, pp. 719-723.
- [10] J. F. Dickson, "On-chip high-voltage generation in MNOS integrated circuits using an improved voltage multiplier technique," *IEEE Journal of Solid-state Circuits*, vol. 11, Issue 3, Jun 1976, pp. 374-378.

- [11] M.-D. Ker, S.-L. Chen, and C.-S. Tsai, "Design of charge pump circuits with consideration of gate-oxide reliability in low-voltage CMOS processes," *IEEE Journal of Solid-state Circuits*, vol. 41, No. 5, May 2006, pp. 1100-1107.
- [12] J.-T. Wu and K.-L. Chang, "MOS charge pumps for low-voltage operation," *IEEE Journal of Solid-state Circuits*, vol. 33, No. 4, April 1998, pp. 592-597.
- [13] J. Shin, I.-J. Chung, Y. J. Park, and H. S. Min, "A new charge pump without degradation in threshold voltage due to body effect," *IEEE Journal of Solid-state Circuits*, vol. 35, No. 8, August 2000, pp. 1227-1230.
- [14] C. C. Wang and J. C. Wu, "Efficiency improvement in charge pump circuits," *IEEE Journal of Solid-state Circuits*, vol. 33, No. 6, June 1997, pp. 852-860.
- [15] T. T. Le, A. v. Jouanne, K. Mayaram, and T. S. Fiez, "Piezoelectric micro-power generation interface circuits," *IEEE Journal of Solid-state Circuits*, vol. 41, No. 6, June 2006, pp. 1411-1420.
- [16] H. Nakamoto, D. Yamazaki, T. Yamamoto, H. Kurata, S. Yamada, K. Mukaida, T. Ninomiya, T. Ohkawa, S. Masui, and K. Gotoh, "A passive UHF RF identification CMOS tag IC using ferroelectric RAM in 0.35- $\mu\text{m}$  technology," *IEEE Journal of Solid-state Circuits*, vol. 42, No. 1, January 2007, pp. 101-110.
- [17] K. H. Edelmoser, and F. C. Zach, "DC-to-DC Converter With Extended Voltage Transfer Ratio, Optimized for Bi-Directional Operation," *WSEAS Transactions on Power Systems*, Issue 6, vol. 1, June 2006, pp. 1057-1061.
- [18] URL: <http://people.equars.com/~marco/poli/phd/node20.html>
- [19] URL: <https://www.eecs.berkeley.edu/~boser/courses/software/spice/CMOS35/index.html>